Autoignition of End Gas in a Rapid Compression Machine under Super Knock Conditions

Yunliang Qi, Yingdi Wang, Hui Liu, Jianxin Wang, Zhi Wang*
State Key Laboratory of Automotive Safety and Energy, Tsinghua University
Beijing, China

1 Introduction

Knock can deteriorate engine performance and even can damage the engine. It is believed that knock is caused by end gas autoignition [1]. For low-intensity knock, the propagation speed of autoignition flame is generally less than the local sound speed, but under certain conditions shock waves can be generated [2]. For high-intensity knock, the propagation speed of autoignition flame can reach or exceed the local sound speed [3], and for the super knock emerged in recent years, the autoignition of end gas may result in detonation [4, 5].

Knock has been observed that autoigniton generally originates from the site near the combustion chamber wall [1-3, 5]. This is because, on one hand, the near wall area is usually the end area in which the mixture has long enough time to prepare autoignition before it is burned by a normal propagating flame. On the other hand, it may also relate to temperature distribution in the vicinity of the wall. When knock occurs, the end gas temperature (calculated based on pressure trace) typically ranges from 750 K to 850 K [6]. This temperature range is just right in the negative temperature coefficient region (NTC) for engine hydrocarbon fuels or their primary reference fuels (PRF). Griffiths et al. [7] suggested that the gas temperature near the wall was less than the central region and was prone to initiate autoignition due to the NTC nature of the fuel. Saijyo et al. [8] also found in their numerical simulation that, in an offset spark case, lower temperature location comes earlier to the autoignition, and they concluded that the differences in the locations of the first autoignition depended on the period during which the local end gas temperatures passed through the region of shorter ignition delay, including the NTC region. However, Pöschl and Sattelmayer [9] believed that NTC did not play any role in the evolution of knock when they investigated the effect of temperature inhomogeneity on knocking combustion in an experiment performed in a rapid compression and expansion machine (RCEM) using PRF fuel. Walton et al. [10] also found that the autoignition of iso-octane/air mixture formed near the wall of a rapid compression facility (RCF) combustion chamber was not attributed to NTC chemistry, and their modeling studies indicated that ignition was not accelerated at the lower temperatures expected in the near-wall region.

Correspondence to: wangzhi@tsinghua.edu.cn

In this study, the autoignition process of the end gas under super knock conditions is investigated. Using a rapid compression machine (RCM), the temperature and pressure conditions corresponding to the top dead center (TDC) of gasoline engines are established. Then the stoichiometric iso-octane/oxygen/nitrogen mixture is ignited after TDC at the center of the combustion chamber using a spark plug. The entire combustion process including the autoignition of the end gas is recorded using high speed photography. Based on the high speed images and the ignition delay evolution of the end gas calculated from the pressure trace, the characteristics of the end gas autoignition and the effect of NTC on the autoignition are analyzed.

2 Experimental Setup and Method

The experimental setup is shown in Figure 1. The stroke of the RCM is 500 mm and the diameter of the combustion chamber is 50.8 mm. The compression ratio can be adjusted by changing the height of the combustion chamber. A spark plug (Denso K20R-U11) was mounted in the circular wall of the combustion chamber, and both the two electrodes of the spark plug were extended so it could ignite the mixture at the combustion chamber center. A pressure sensor (Kistler 6125C) was flush mounted at the position opposite the spark plug. The pressure signal was amplified using Kistler 5018. The left end of the combustion chamber had a quartz glass window with an effective diameter of 50.8mm which allowed optical access to the full combustion chamber area.

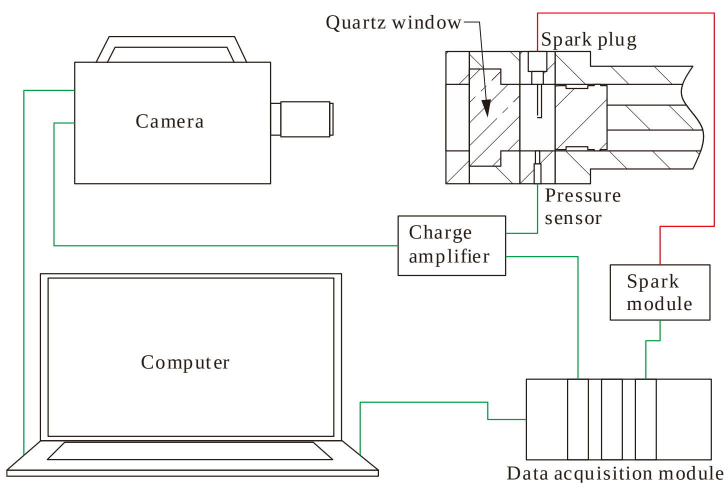

Figure 1. Schematic of experimental setup

A high speed camera (Photon SA-X2) was used to capture the natural flame luminosity directly at 288 k frames per second with a lens of Nikon Micro Nikkor 1: 2.8G. The shutter and aperture and other parameters were adjusted in different test conditions to make the image brightness not too low or not saturated at the time of autoignition onset. The camera shooting and the spark ignition were triggered by a preset pressure threshold, and their synchronization was made by a NI data acquisition system. The ignition timing was set within 1 ms after the end of compression (EOC). Tests show that this ignition timing had very small influence on the experimental repeatability [11].

Iso-octane was used as the fuel, and the other parts in the stoichiometric mixture were N_2 and O_2 at a molar ratio of 1: 3.76. The initial temperature was equal to the ambient temperature, which was 302 K±2 K.

3 Results and Discussion

3.1 Autoignition process of the end gas

Figure 2 shows the pressure trace after the spark ignition under the conditions of T_{EOC} = 641 K and p_{EOC} = 2.5 MPa. The corresponding high speed images at some certain timings are shown in Figure 3. It can be seen in Figure 2 that, at t_{ASI} = 8.29 ms or so, the pressure trace has a sudden and sharp rise, and at the same time, as shown in Figure 3, a brighter area emerges at the upper left corner of the combustion chamber, which indicates that an end gas autoignition event occurs. Then, the autoignition flame continues propagating into the other unburnt area and gets brighter. Only 0.1 ms later, at t_{ASI} = 8.30 ms, the speed of autoignition flame front reaches to about 1840 m/s, indicating the autoignition has developed into a detonation wave. After the completion of the combustion, violent pressure oscillation is formed in the combustion chamber with peak pressure exceeding 20 MPa and oscillation amplitude exceeding 10 MPa, which is the typical characteristics of super knock.

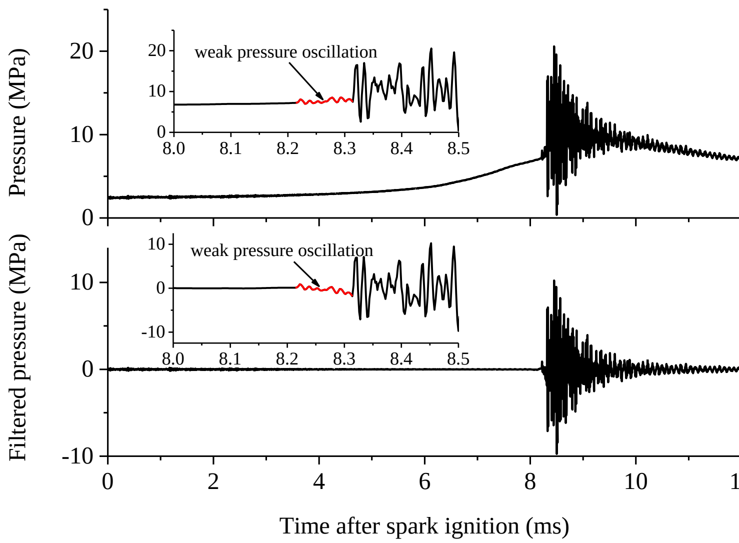

Figure 2. Pressure trace after spark ignition (T_{EOC} = 641 K and p_{EOC} = 2.5 Mpa)

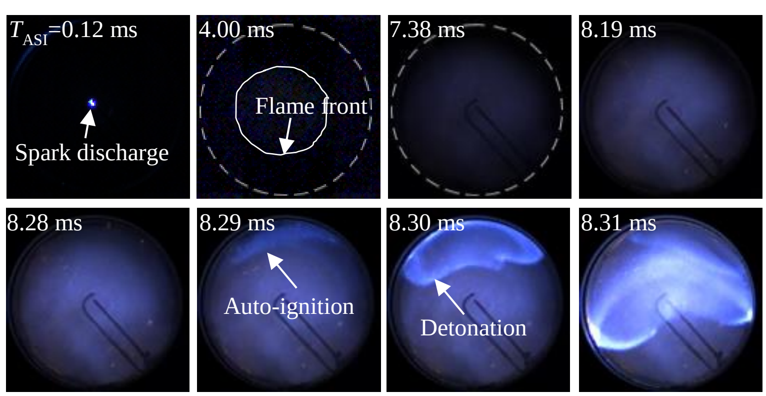

Figure 3. High speed combustion images at some certain timings (shutter=0.248 μs)

Before the violence autoignition at t_{ASI} = 8.29 ms, a relatively mild autoignition is also found at t_{ASI} = 8.19 ms. The pressure trace in Figure 2 clearly shows a slight pressure oscillation starting from t_{ASI} = 8.22 ms, of which oscillation amplitude is about 0.7 MPa and the oscillation duration is about 0.1 ms. However, this autoignition can only make very small change of image luminosity which is difficult to be recognized by naked eye in still images. To clearly show this autoignition process the images are processed using background subtraction and 10 times enhancement, which is given in Figure 4 together with the corresponding pressure trace. It can be seen that, at the time of the Image (a), a slight increase in brightness occurs in the upper right corner of the combustion chamber, which slightly offsets from the detonation initiation position as shown in Figure 3 (t_{ASI} = 8.29 ms). Then brightness area expands to the surroundings. Because of the very low intensity, this slight brightness increase should be caused by low temperature reaction of the end gas. This spontaneous reaction does not immediately develop into high temperature reaction like the knock onset process observed in optical engines in previous literatures [2, 3, 6, 9]. This may due to that the mean temperature of the unburned zone in the combustion chamber is relatively low (about 813 K calculated thermodynamically based on pressure trace using the common used method for RCM test [12]) and the pressure wave caused by the spontaneous low temperature reaction is not intensive enough to significantly raise the temperature and pressure of the surrounding mixture to induce a high temperature reaction. Therefore, this brighter area can be considered as a result of the sweep by the pressure wave originating from the spontaneous reaction at t_{ASI} = 8.19 ms. By the time of Image (d), the pressure wave front has developed into a nearly circular shape and has been into the burned area. At the time of Image (h), the pressure wave front reaches the lower left wall then continues to oscillate in the combustion chamber. The propagation velocity of the pressure wave estimated from the images is about 1005 m/s, which is slightly larger than the sonic velocity (986 m/s) calculated using the experimental conditions, so the pressure wave is confirmed to be a shock wave.

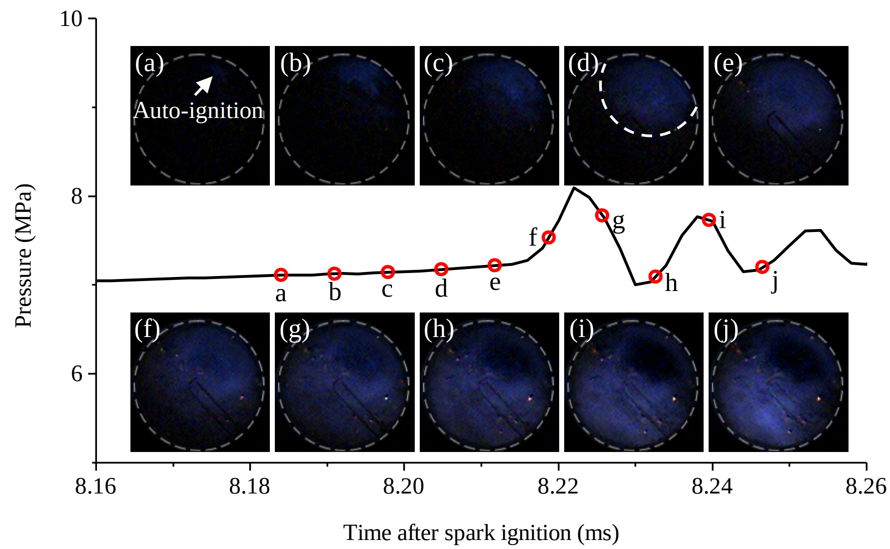

Figure 4. High speed combustion images at some certain timings (shutter=0.248 μs) and the correspondence to pressure trace

3.2 Ignition delay evolution of end gas

The ignition delay evolution of the end gas for the above case is shown in Figure 5, and two more cases with the same p_{EOC}=2.5 MPa but different T_{EOC} (681 K and 729 K, respectively) are also presented for comparison. To obtain the ignition delays in an evolution curve, the temperature trace was calculated firstly using the method mentioned in Ref. [12]. Then, the ignition delay was calculated using Chemkin software for each point in the pressure trace together with the calculated corresponding temperature. The time range of the ignition delay evolution curves shown in Figure 5 is from the start of spark ignition to the initiation of detonation. The gray lines in Figure 5 are ignition delays of the stoichiometric iso-octane/O_2/N_2 mixture at different initial pressures from 2.0 MPa to 9.5 MPa with an interval of 0.5 MPa. The PRF reaction mechanism developed by Ra et al. [13], which shows more applicability for this study than the detail mechanism in our previous works [11], is used to do the calculation. Since Ra's mechanism is a reduced one, the NTC phenomenon is not obvious in the calculated results, but NTC trend can still be observed for low pressure conditions (for example, the pressures less than 3.0 MPa). It can be seen that for the case shown in Figure 2 (T_{EOC}=641 K), the ignition delay evolution curve of the end gas almost doesn't pass through the NTC region. For the other two cases, only a small part of ignition delay evolution curve passes through the NTC region. Therefore, the NTC property of iso-octane has limited effect on end gas autoignition under the conditions used in this study.

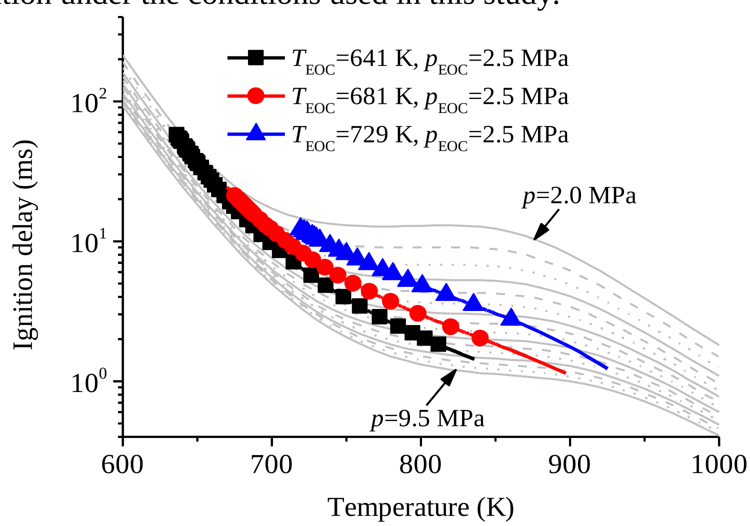

Figure 5. Ignition delay evolution of end gas after spark ignition

4 Conclusions

Super knock (detonation) is generated using spark ignition induced end gas autoignition for stoichiometric iso-octane/O_2/N_2 mixture in a rapid compression machine. The combustion process is recorded by high speed photography synchronizing with pressure data acquisition. Through the analysis of the combustion image and the pressure trace, the following conclusions can be drawn.

1. Two autoignition events with very short time interval are sequentially observed in end gas area, which has not been reported in previous engine researches. The first autoignition can generate

a weak shock wave propagation in the combustion chamber, and the second autoignition can lead to a detonation.

2. The ignition delay evolution curve of the end gas almost does not pass through the NTC region for lower temperature condition (T_{EOC} = 641 K), and only a small parts of ignition delay evolution curves pass through the NTC region for higher temperature conditions (T_{EOC} = 681 K and T_{EOC} = 729 K). Therefore, in this study, the effect of NTC on the end gas autoignition is not significant.

This work was supported by National Natural Science Foundation of China (No. 91541206).

References

1. J. Heywood, Internal combustion engine fundamentals, McGraw-Hill Education, New York, 1988, p.
2. T. Hayashi; M. Taki; S. Kojima; T. Kondo, SAE Technical Paper 841336 (1984)
3. B. Stiebels; M. Schreiber; A. S. Sakak, SAE Technical Paper 960827 (1996)
4. G. T. Kalghatgi; D. Bradley, International Journal of Engine Research 13 (4) (2012) 399-414.
5. Y. Qi; Z. Wang; J. Wang; X. He, Combustion and Flame 162 (11) (2015) 4119-4128.
6. G. Konig; C. G. W. Sheppard, SAE Technical Paper 902135 (1990)
7. J. F. Griffiths; B. J. Whitaker, Combustion and Flame 131 (4) (2002) 386-399.
8. K. Saijyo; K. Nishiwaki; Y. Yoshihara, JSME international journal. Ser. B, Fluids and thermal engineering 46 (1) (2003) 44-51.
9. M. Pöschl; T. Sattelmayer, Combustion and Flame 153 (4) (2008) 562-573.
10. S. M. Walton; X. He; B. T. Zigler; M. S. Wooldridge; A. Atreya, Combustion and Flame 150 (3) (2007) 246-262.
11. Y. Qi. Experimental Research on Super Knock Mechanism of Gasoline Engine (in Chinese). Tsinghua University, Beijing, 2015.
12. X. He; M. T. Donovan; B. T. Zigler; T. R. Palmer; S. M. Walton; M. S. Wooldridge; A. Atreya, Combustion and Flame 142 (3) (2005) 266-275.
13. Y. Ra; R. D. Reitz, Combustion and Flame 155 (4) (2008) 713-738.